Standard Model Physics at the LHC

J. Mnich

III. Phys. Inst. B, RWTH Aachen, Germany

Received 3 August 2004;
final version 15 September 2004

In addition to the large discovery potential for Higgs bosons and new physics phenomena, like for instance Supersymmetry, the experiments at the LHC will also be able to perform precise measurements of many Standard Model processes. The huge cross sections and the high collision energy will allow the exploration of less well tested areas of the model and to improve significantly on the precision of many parameters. Therefore the detailed experimental study of known Standard Model processes at the LHC will not only prepare the anticipated discoveries but also complement their interpretation. This article describes some selected items on the perspectives of the two general purpose detectors ATLAS and CMS on the determination of parton distribution functions, tests of QCD and electroweak physics at the highest energies and the physics of the top quark.

PACS: 62.20
Key words: LHC, Standard Model

1 Introduction

The Large Hadron Collider (LHC) under construction at CERN in Geneva combines the two most important virtues for high energy physics experiments. From the year 2007 it will provide proton-proton collisions at the highest centre-of-mass (cms) energy of 14 TeV and large luminosities in the range from 10^{33} cm^{-2}s^{-1} in the initial phase up to 10^{34} cm^{-2}s^{-1} at a later stage.

Cross sections of various Standard Model (SM) processes in $p\bar{p}$ and pp collisions as a function of the energy are compared in the left part of Fig. 1 [1]. For instance because of the higher energy at the LHC the production cross sections for the heavy gauge bosons W and Z and $t\bar{t}$ quark pairs are significantly larger than at the Tevatron. Already during the low luminosity phase of the LHC this results in large production rates as can be seen from the right scale of this plot. Approximately 200 W, 50 Z bosons and one $t\bar{t}$ pair will be produced every second. Even when taking into account reasonable values for selection efficiencies and the branching ratios into clean leptonic final states (e and μ) it is evident from these numbers that large data samples will be acquired very shortly after the start-up of the collider. Besides providing excellent means to calibrate and understand the detectors these data samples will allow many precision measurements.

2 Parton distribution functions

Most of the interesting reactions at the LHC are hard scattering processes of the partons inside the protons. Therefore the accurate knowledge of the parton

Fig. 1. Left: Cross sections of various SM processes in (anti)proton-proton collision in the Tevatron and LHC energy ranges. Right: LHC area of interest in the $x - Q^2$-plane of the scattering partons compared to the regions accessible at HERA and fixed target experiments.

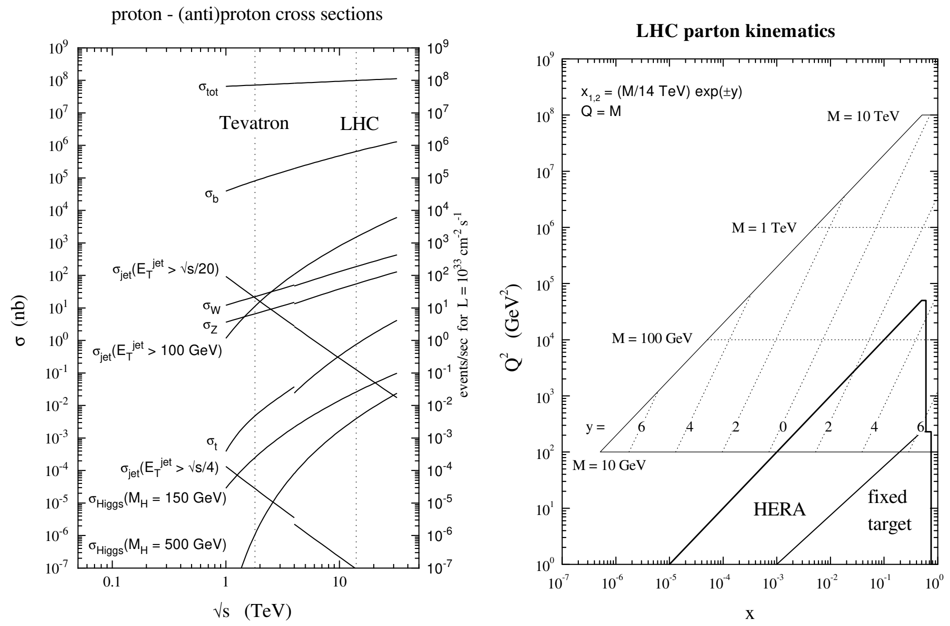

distribution functions (PDF) of quarks, anti-quarks and gluons is mandatory for the interpretation of the data. The region of the fractional parton momentum x and the momentum transfer Q^2 interesting for LHC physics is shown in the right part of Fig. 1. This is compared to the area investigated by fixed target experiments and at the electron-proton collider HERA. As the overlap of both regions are small theoretical models like the DGLAP evolution [2] are required to extrapolate from the experimentally tested regions of low Q^2 to the higher momentum transfers important for the LHC physics. It is therefore desirable to determine the PDFs for all parton species directly from LHC data and to test the extrapolation models and to improve the precision.

SM processes provide various means to measure and constrain the PDF through differential distributions like the transverse momentum p_T and the pseudo-rapidity η. An example for a particular sensitive observable is the cross section ratio of W^+ to W^- bosons which is sensitive to the ratio of u- and d- quarks in the proton. The expected ratio of positively to negatively charged electrons and muons as a function of rapidity from selected $W^\pm$-decays is shown on the left hand side of

Fig. 2. Left: Ratio of positive to negative leptons (e, μ) as a function of the absolute rapidity $|\eta|$ from W boson decays. Right: Transverse momentum spectrum of muons in jets from events with an isolated photon.

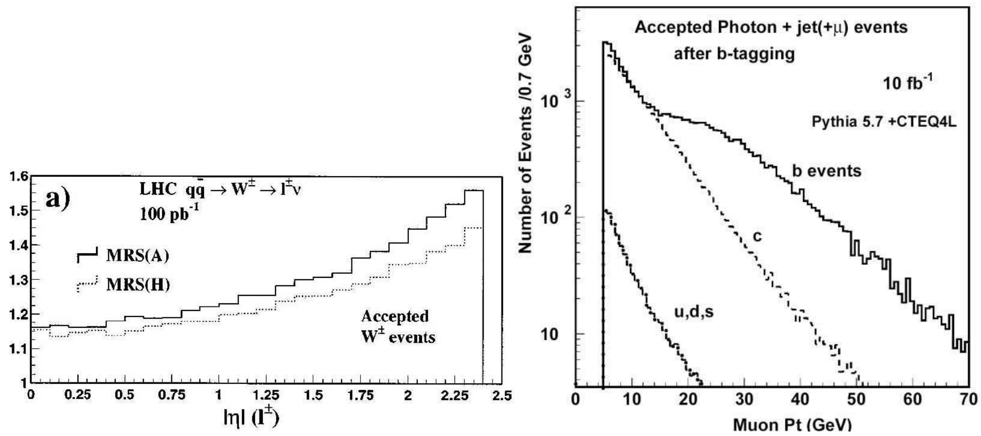

Fig. 2. The two curves are obtained from sets of PDFs with small differences in the sea quark distribution [3]. The very low integrated luminosity of 0.1 fb^{-1} which can be collected in a few days at initial LHC conditions distinguishes between these models.

Another example are the PDFs of s,c and b quarks which can be determined from the quark-gluon scattering processes gb $\to$ bγ, gc $\to$ cγ and gs $\to$ cW. Tagging of the final states should be possible by exploiting the clear signature of isolated photons or W bosons accompanying the jet. The jets of b- and c-quark are identified through displaced vertices and their leptonic decays. Fig. 2 shows the p_T-spectrum obtained from a generator level study of final states with isolated photons and jets [4]. It should be noted that these analyses are particularly suited for the initial low luminosity phase as the pile-up of collisions in one bunch crossing is small. However the feasibility of these analyses still has to be demonstrated taking into account full detector and background simulations.

Other SM reactions will contribute to the determination of PDFs. A list of promising channels is given in Tab. 1.

3 QCD and Jet Physics

Hadron colliders are a predestined tool for probing strong interactions and the physics of jets. The observable spectrum of transverse jet energies E_T ranges from about 200 GeV to several TeV with the corresponding cross sections varying over

Table 1. List of final states of SM processes and their ability to constrain parton distribution functions.

Process:	PDF constraint on:
di-jets	quarks & gluons
jet + photons	quarks & gluons
jet + W boson	quarks & gluons
W & Z bosons	quarks
Drell-Yan	quarks

Fig. 3. ATLAS studies of jet physics and QCD [5]. Left: Differential cross section of the transverse jet energy. Right: Running of α_s obtained from this spectrum.

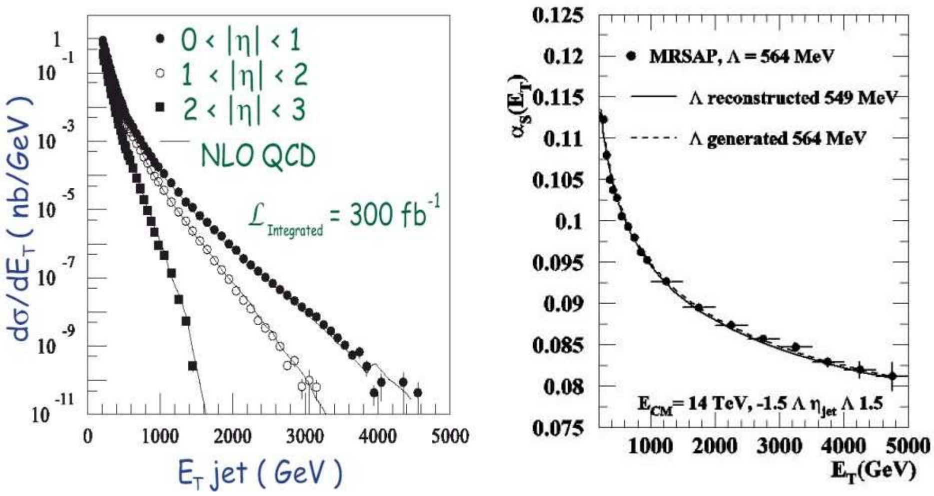

11 orders of magnitude. This is illustrated in Fig. 3 showing the differential cross section $\mathrm{d}\sigma/\mathrm{d}E_T$ in various intervals of rapidity. Of particular interest are the jets at the highest energies. For an integrated luminosity of 300 fb^{-1} which corresponds to a few years of LHC operation at the highest luminosity about 4 million jets with $E_T > 1$ TeV and still 400 with $E_T > 3$ TeV are expected per experiment [5]. These samples will allow to probe QCD at the smallest distance scales and provide information on a possible quark substructure..

The observed jet spectrum can be used to extract the strong coupling constant α_s. However, the absolute precision on $\alpha_s(m_Z)$ from this method will be limited to approximately $\pm 10\%$ because of the uncertainties on PDFs, the renormalisation and factorisation scale as well as the parametrisation of the E_T spectrum in terms of α_s [5]. Nevertheless from the measured jet spectrum the running of α_s can be demonstrated from energy scales of about 100 GeV investigated at previous colliders up to a few TeV. This is illustrated in the right part of Fig. 3.

4 Electroweak Physics

The LHC will abundantly produce W and Z bosons which through their leptonic decays provide relatively clear signatures and are readily identifiable. The experiments will hence be able to study the properties of W and Z bosons and to complement and extend the test of the electroweak theory performed so far at e^+e^-- and $p\bar{p}$-colliders.

An important parameter for precision tests of electroweak theory is the mass of the W boson [6]. Techniques to measure this parameter at hadron colliders have been developed and already today the Tevatron experiments provide results competitive to the precision reached at LEP. At the LHC the overwhelming statistics on Z-bosons can be used to experimentally constrain theoretical uncertainties on the production and to determine accurately the detector response in the leptonic decay channels. This will minimise the dependence on Monte Carlo simulations and the corresponding uncertainties. A study from the ATLAS experiment [7] shows that a total error $\Delta m_{\mathrm{W}} \leq 25$ MeV per channel and experiment is obtainable. Therefore it is believed that the LHC will further improve the error on m_{W} beyond the anticipated uncertainty of about 20 MeV from final LEP and Tevatron Run II data.

A first example is the Drell-Yan process $q\bar{q} \to e^+e^-, \mu^+\mu^-$ which constiutes in some sense the equivalent of the reaction $e^+e^- \to$ hadrons which was extensively studied at LEP and SLC. This process is not only an important tool to constrain the PDFs but also the discovery channels for heavy new particles decaying into leptons, e.g. a Z' boson. Fig. 4 shows the expected number of events per di-lepton channel and experiment as a function of the mass for a total luminosity of 100 fb^{-1} in comparison to the expectation at the Tevatron Run II (10 fb^{-1}) [1, 8]. The higher luminosity and energy at the LHC will extend the sensitivity well beyond the reach of the Tevatron into the TeV range.

In addition to the cross section also the forward-backward asymmetry A_{FB} in Drell-Yan lepton-pair production can be measured. The ambiguity of the direction of the incoming quark and anti-quark in pp-collisons is resolved assuming that the anti-quark is usually the parton with the lower x value. The right half of Fig. 4 shows the result of an ATLAS study for $q\bar{q} \to e^+e^-$ at the Z-pole [9]. As it was done in e^+e^--experiments this A_{FB} measurement can be turned into a measurement of the effective weak mixing angle $\sin^2\theta_W$. Provided that electrons in the forward region can be identified reliably a statistical error of $\Delta\sin^2\theta_W \approx 1.4 \cdot 10^{-4}$ is expected for 100 fb^{-1}. Further studies are needed to estimate if systematic errors from the limited knowledge of the PDFs, lepton acceptance and radiative corrections can be controlled to the required level such that this measurement will become significant.

The high energy makes the LHC also an ideal place to study di-boson production

Fig. 4. Left: Expected number of di-lepton events in 50 GeV bins per channel and experiment. Right: Forward-backward asymmetry at the Z pole in $q\bar{q} \to e^+e^-$ as a function of rapidity for two sets of electron acceptance.

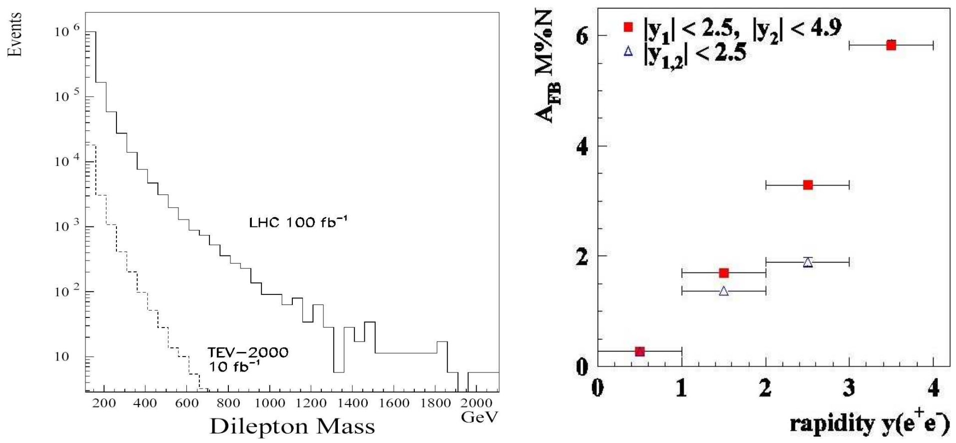

from which information on the triple gauge boson vertices can be deduced. In the SM two such vertices, $WW\gamma$ and WWZ exist whereas all others, in particular those involving only the neutral bosons γ and Z, do not.

The $WW\gamma$ vertex is tested in $W\gamma$ final states and a sensitive variable is the transverse momentum of the photon of which an example is shown in Fig. 5. Deviations from the SM are described by the parameters λ and $\Delta\kappa$ which have been found to be consistent with zero at the percent level at LEP from studies of W pair production $e^+e^- \to W^+W^-$. From this analysis limits on the coupling parameters can be derived as shown in the right part of the figure. In particular the sensitivity to λ is much higher at the LHC because deviations from the SM induced by this coupling scale with the square of the cms energy.

Likewise $Z\gamma$ will be used to observe anomalous $ZZ\gamma$ and $Z\gamma\gamma$ couplings. The observable effects of these vertices grow even stronger, $\propto s^{3/2}$ or even $\propto s^{5/2}$, with the cms energy. Differential cross sections for two sensitive observables, the photon transverse momentum and the invariant mass of the $\ell^+\ell^-\gamma$ system, are shown in Fig. 6. Expectations from SM background processes are compared to anomalous couplings taking the two parameters h_1 and h_2 as an example at their current experimental bounds. The increase in cross section and the distortions of the spectra are large such that anomalous couplings small to todays limits would readily be observed at the LHC.

In the SM also vertices with four gauge bosons exits. These quartic couplings contribute to final states with three bosons. However, final states of three heavy

Fig. 5. Test of the WWγ vertex [10]. Left: Photon p_T spectrum in selected Wγ final states for SM couplings (filled histogramm) and for coupling parameters λ and $\Delta\kappa$ consistent with current limits. Right: Limits in the plane $\lambda - \Delta\kappa$ obtainable for various integrated luminosities.

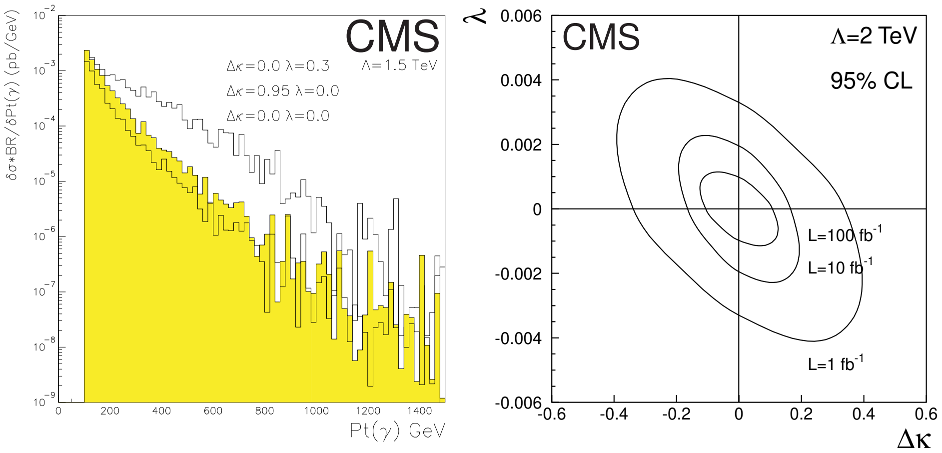

Fig. 6. Differential cross sections of selected Zγ final states for SM backgrounds and anomalous couplings h_1 and h_2 at current limits [11]. Left: Transverse photon momentum. Right: Invariant mass of the photon and the lepton pair from the Z decay.

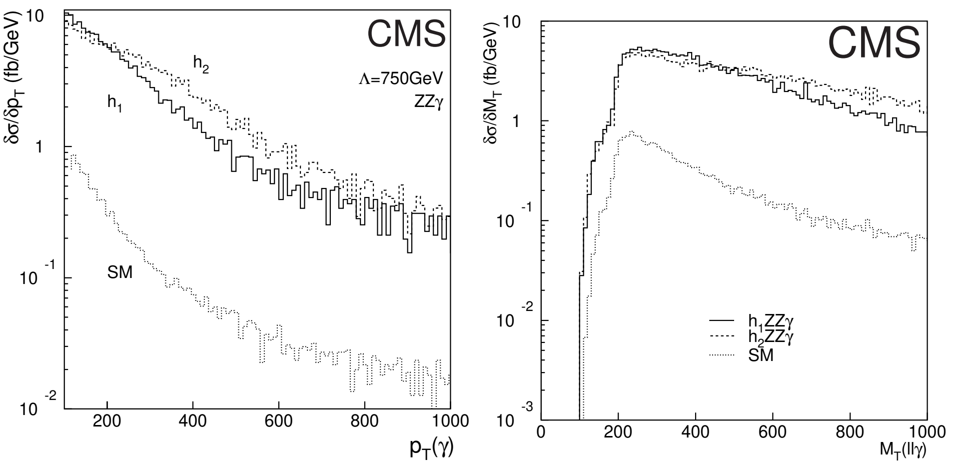

Fig. 7. Left: ATLAS simulation for the SM expectation of the transverse momentum spectrum in selected $W\gamma\gamma$ final states for 30 fb^{-1}. Right: Impact of anomlaous quartic coupling constants to the spectrum [14].

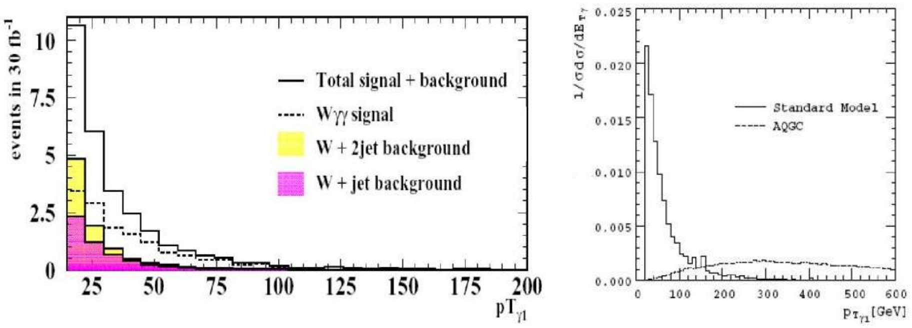

bosons are difficult to observe due to several neutrinos from leptonic W decays, e.g. $pp \to WWW + X$, or because of low cross sections like for $pp \to ZZW + X$ [12, 13]. Therefore the easiest channel to observe quartic gauge boson couplings is $pp \to W\gamma\gamma + X$. The left part of Fig. 7 shows the expected transverse momentum spectrum for the SM signal and background proving that the quartic $WW\gamma\gamma$ coupling is observable. Anomalous contributions to it would be observable as an increase in the cross section at high p_T values. This is illustrated in the right part of the figure [14].

5 Physics of the Top Quark

Because of the high luminosity and cross section the LHC turns out to be a real top factory which will permit precision measurements of the properties of the heaviest SM fermion. Contrary to the Tevatron the dominant production process for top quark pairs is gluon fusion $gg \to t\bar{t}$ contributing with about 87% much more than quark annihilation $q\bar{q} \to t\bar{t}$. The top quark decay to almost 100% into a b-quark and a W boson such that the signature of a $t\bar{t}$ pair is given by the decay topology of the W pair in addition to the two b-quarks in the final state.

An important example is the measurement of the top quark mass which is a crucial quantity for precision tests of the SM as it enters quadratically in quantum corrections. The most evident channel for a precise top mass measurement is the semi-leptonic final state where one W decays hadronically and the other into an electron or muon. It provides a clear signature from the high momentum lepton together with a high branching ratio and full mass information from the hadronically decaying top quark. The top mass is then reconstructed from the two light quark jet exploiting a W mass constraint and one of the b-quark jets.

Fig. 8 shows two such invariant mass distributions from the experiments [15, 16].

Fig. 8. Reconstructed top mass distribution in the semi-leptonic channel from ATLAS and CMS analyses.

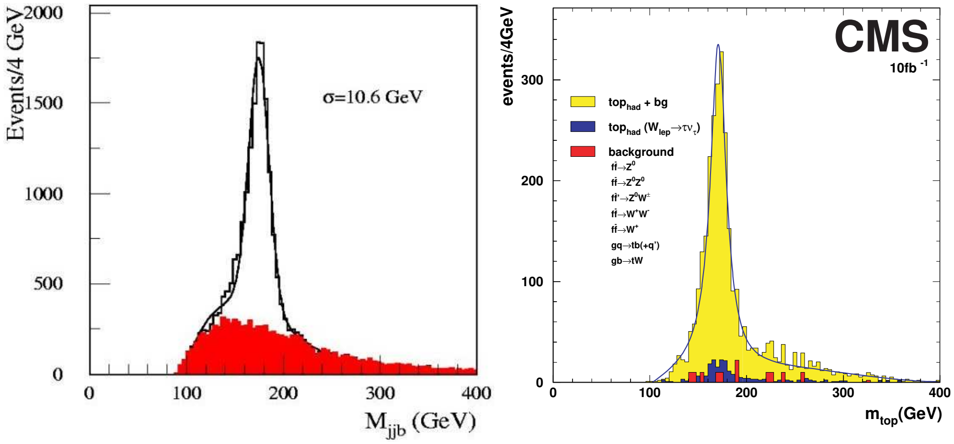

Very clean top samples can be obtained in this channel where the signal to background ratio can be adjusted by the selection criteria. This is the main reason for the different signal to background ratios in Fig. 8. This offers the possibility to optimise the analysis for the available integrated luminosity balancing statistical and systematic errors and to obtain a significant result for the top mass rather quickly. The achievable ultimate precision from this channel is expected to be $\Delta m_{\rm t} \approx 1$ GeV where the knowledge of the energy scale of b-quark jets and of final state radiation will be the main limiting factors.

Also the other decay modes of $\mathrm{t\bar{t}}$ will contribute to the top mass determination. The fully hadronic decay mode has a large branching ratio of 45% but the six jets in the final state create a difficult environment and ambiguities. Fig. 9 (left) shows a sample mass spectrum from an ATLAS analysis [15] which estimates a precision of $\Delta m_{\rm t} \approx 3$ GeV. In 11% of the cases the W pair decays into two leptons. The decays into electrons or muons provide a very clean sample. Even though the presence of the two neutrinos prohibits the full kinematic constraint of the events information on the top mass can be extracted. Eventually this results in a significant mass measurement with an error of $\Delta m_{\rm t} \approx 1.7$ GeV from this channel [15].

Another interesting mode for the mass measurement are top decays where a J/Ψ meson emerges from the b fragmentation and the W decays into an electron or muon. The J/Ψ is readily identifiable by its decay into two muons and the invariant mass of the J/Ψ and the lepton from the W decay is rather sensitive to $m_{\rm t}$ as can be seen from the right part of Fig. 9 [17]. The partially reconstructed top mass is independent of the b jet energy scale thus circumventing the problem limiting

Fig. 9. Left: Reconstructed top mass spectrum from selected full hadronic top pair decays [15]. Right: Dependence of the reconstructed mass of the lepton-J/Ψ system on the top quark mass (solid line) compared to the sensitivity on the lepton pair mass in two lepton decays [17].

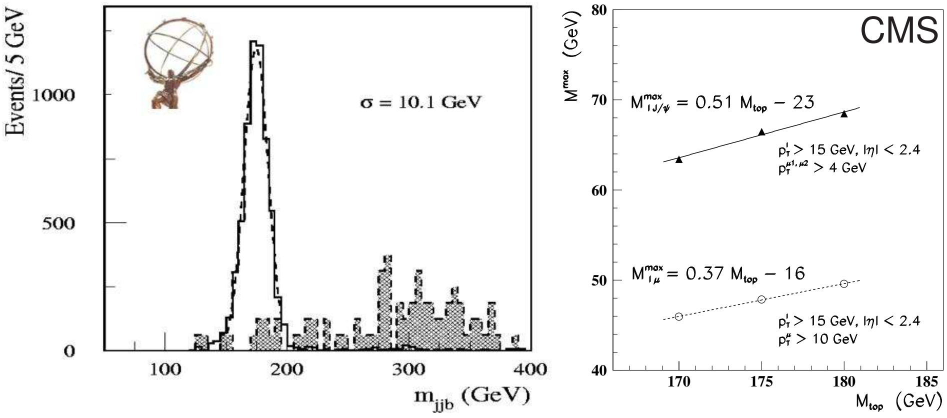

the precision of the inclusive semi-leptonic channel. This method needs a higher integrated luminosity because of the low branching ratio and it will ultimately be limited by the knowledge of the b fragmentation function. However with about 1000 events per year at a luminosity of 10^{34} cm^{-2}s^{-1} a final precision of $\Delta m_{\rm t} \approx 1$ GeV per experiment is expected making this a very promising analysis.

Top decays offer the interesting possibility to study W bosons in the longitudinal polarisation state which exists only for massive bosons. The SM predicts that 70% of the W are in this state with the rest being left-handed because in the limit of a vanishing b quark mass the W cannot be right-handed. The fraction of longitudinally polarised to left-handed W bosons is given by $m_{\rm t}^2/2m_{\rm W}^2$ demonstrating that this phenomena is intimately connected to the large Yukawa coupling of the top and therefore the Higgs mechanism. First measurements are obtained at the Tevatron [18]. Other sources of longitudinally polarised W bosons are the reaction $\rm e^+e^- \to W^+W^-$ investigated at LEP and if kinematically allowed Higgs decays $H \to \rm W^+W^-$.

A sensitive W spin analyser in top decays is the angle θ^* between the charged lepton in the W rest frame and the W in the top rest frame [19]. The left part of Fig. 10 shows the angular distribution on generator level for the two W polarisation states. Because the lepton momentum in the detector is strongly correlated to the angle θ^* the spectrum is distorted after event selection. Nevertheless using the semi-leptonic top pair decays from the modest integrated luminosity of 10 fb^{-1}

Fig. 10. Left: Distribution of the angle θ^* between the charged lepton in the W rest frame and the W in the top rest frame on generator level for the two possible W polarisation states. Right: Double differential distribution of the lepton angles in the top quark rest frames after detector simulation and acceptance corrections.

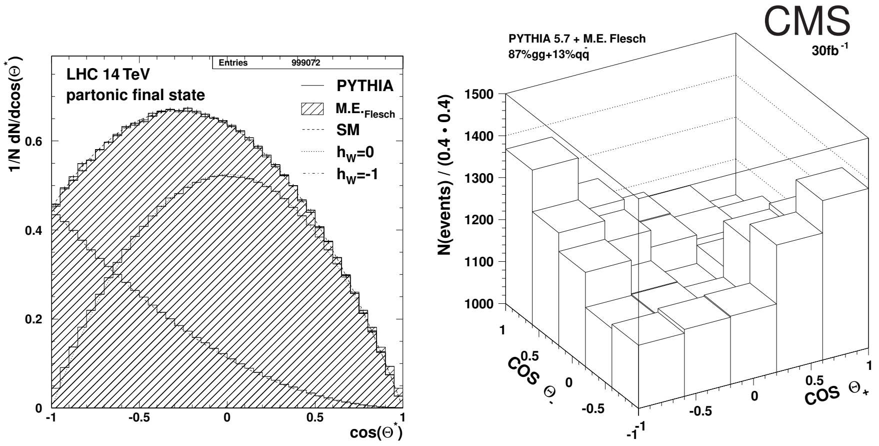

the fraction of longitudinally polarised W boson can be measured with a total uncertainty of approximately ± 0.03.

The production of top pairs at the LHC offers the unique opportunity to study the spin of a quark at production. Because of its high mass the lifetime of the top is very short such that no bound hadron states form and the information on the top quark spin is preserved until its decay. The $\mathrm{t\bar{t}}$ spin correlation A is defined as the asymmetry of finding top and anti-top in the same or in different polarisation states:

$$A = \frac{N(\mathrm{t}_L\bar{\mathrm{t}}_L + \mathrm{t}_R\bar{\mathrm{t}}_R) - N(\mathrm{t}_L\bar{\mathrm{t}}_R + \mathrm{t}_R\bar{\mathrm{t}}_L)}{N(\mathrm{t}_L\bar{\mathrm{t}}_L + \mathrm{t}_R\bar{\mathrm{t}}_R) + N(\mathrm{t}_L\bar{\mathrm{t}}_R + \mathrm{t}_R\bar{\mathrm{t}}_L)}\,.$$

This quantity is sensitive to the production mechanism because different spin correlations are expected for the t-channel gluon fusion process ($A = +0.43$) and the s-channel quark annihilation ($A = -0.47$) [19]. Since the gluon fusion dominates a combined value of $A = 0.31$ is predicted at the LHC.

Here the angle of the charged lepton in the (anti)-top rest frame can be used as spin analyzer. The double differential distribution of $\theta^*_\pm$ for the positive and negative lepton in di-lepton events as shown in Fig. 10 is obtained. From di-leptonic $\mathrm{t\bar{t}}$ events in 30 fb^{-1} a precision of $\Delta A \approx 0.04$ can be obtained.

Evidently the determination of the total cross section $\mathrm{pp} \to \mathrm{t\bar{t}}$ at 14 TeV is an important and interesting measurement in itself. Moreover as it depends quadratically on m_t it can provide another handle on the top mass provided that the experimental, namely on the luminosity, and theoretical uncertainties can be con-

Fig. 11. Left: Invariant mass distribution of the top quark pair in the presence of a hypothetical resonance at 1.6 TeV decaying into $\mathrm{t\bar{t}}$ [7]. Right: Expected transverse momentum spectra of photons in selected $\mathrm{t\bar{t}}\gamma$ events for two top quark charge assignments [20].

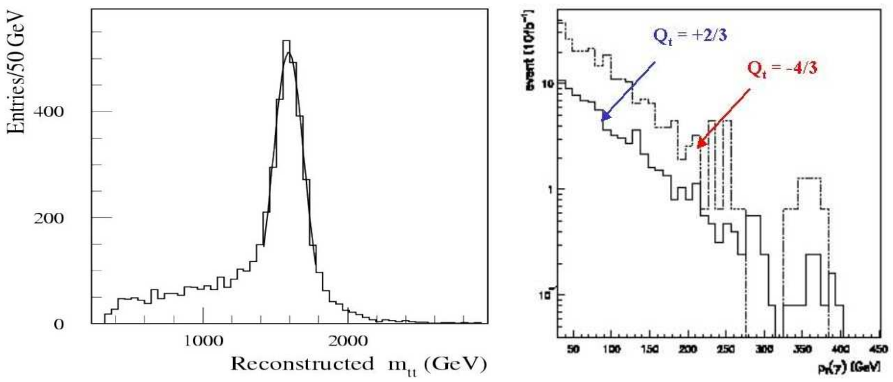

trolled to the percent level. Also precise measurements of differential cross sections as $\mathrm{d}\sigma_{\mathrm{t\bar{t}}}/\mathrm{d}p_T$ and $\mathrm{d}\sigma_{\mathrm{t\bar{t}}}/\mathrm{d}\eta$ are very valuable as they constrain quark and gluon PDFs at high Q^2 values and help to reduce uncertainties on discovery channels like Higgs and SUSY production channels.

Of particular interest is also the invariant mass distribution of the $\mathrm{t\bar{t}}$ system. A hypothetical particle decaying preferentially into the heaviest SM particle would show up as a resonance in the differential cross section $\mathrm{d}\sigma_{\mathrm{t\bar{t}}}/\mathrm{d}m_{\mathrm{t\bar{t}}}$. The result of an ATLAS simulation is shown in the left part of Fig. 11 for a 1.6 TeV particle [7]. In the absence of such a resonance stringent limits can be set.

The SM charge assignment $Q_t = +2/3$ has not yet been unambiguously established experimentally through the charge determination of the two decay products in $\mathrm{t} \to \mathrm{W^+b}$. That is the hypothetical value $Q_t = -4/3$ and the subsequent decay $\mathrm{t} \to \mathrm{W^-b}$ has not been excluded. One way would be to measure the lepton charge from the W decay and to distinguish a b-quark from a $\mathrm{\bar{b}}$ with a jet charge determination. The investigation of $\mathrm{t\bar{t}}\gamma$ events offer a more elegant method to distinguish between the two possibilities. Final state photon radiation would take place more likely if the absolute charge is larger. This is illustrated in the right part of Fig. 11 which shows the photon spectra for the two cases expected for 10 fb^{-1} integrated luminosity [20].

The large available statistics at the LHC will allow to search for rare decays of the top quark. Such analyses comprise rare SM decays such as the CKM suppressed modes $\mathrm{t} \to \mathrm{W^+s}$, $\mathrm{W^+d}$ and the higher order processes $\mathrm{t} \to \mathrm{W^+Zb}$, $\mathrm{t} \to \mathrm{W^+W^-c}$ as well as flavor changing neutral current decays like $\mathrm{t} \to \mathrm{cZ}$.

In addition to the $\mathrm{t\bar{t}}$ pairs single top quarks can be produced in pp-collisions. Various production mechanisms all involving the Wtb-vertex add up to a significant cross section. Its measurement therefore allows the direct determination of the V_{tb} matrix element of the CKM matrix. The first observation of this process is expected at the Tevatron during the ongoing Run II. Experimentally single top events are identified by leptonic decays of the W boson and $\mathrm{t\bar{t}}$ production, together with $\mathrm{Wb\bar{b}}$ final states, turn out to be the most important sources of background. Altogether it is believed that V_{tb} can be measured to the few percent level.

6 Conclusions

The general purpose experiments ATLAS and CMS will have a large physics potential not only for discovery of new physics phenomena but also for precise test of the SM in known channels. The high energy and luminosity of the LHC will offer the possibility to explore a new energy domain and to acquire large data sets of processes which today lack of statistics.

In particular in the initial phase of the experimental programme the investigation of SM processes will be indispensable to understand the sophisticated detectors, to reduce at the relevant energy scale the theoretical uncertainties on QCD and PDF and this way prepare the basis for the anticipated discoveries. Careful studies of SM reactions can be used to understand and normalize Monte Carlo generators which are needed in combination with data to understand the backgrounds to new physics.

Beyond that the LHC opens many possibilities for precise tests of the SM of which important examples are discussed above and which are completing its discovery potential. Because of the large event rates most of the SM analysis will be limited by systematic uncertainties. To achieve the optimum precision it will be important to develop and to explore different techniques for the measurements.

Acknowledgements

I would like to thank the organisers of the workshop for the invitation and their hospitality and I am grateful to my colleagues at ATLAS and CMS for providing me with results and information on their analyses. The author is supported by the german Bundesministerium für Forschung und Technologie.

References

[1] Workshop on Standard Model Physics (and more) at the LHC, CERN Yellow Report 2000-004.

[2] G. Altarelli and G. Parisi, Nucl. Phys. 126 (1977) 297; V.N. Gribov and L.N. Lipatov, Sov. J. Nucl. Phys. 15 (1972) 438 and 675; Yu. L. Dokshitzer, Sov. Phys. JETP 46 (1977) 641.

[3] M. Dittmar, F. Pauss, and D. Zürcher, Phys. Rev. D56 (1997), 7284.

[4] M. Dittmar, K. Mazumdar, CMS NOTE-2001/002.

[5] H. Stenzel, ATLAS, ATL-PHYS-2001-003.

[6] U. Baur et. al., hep-ph/0202001.

[7] ATLAS Detector and Physics Performance, Technical Design Report, CERN/LHCC 99-14.

[8] D. Bourilkov, Proc. 30th Int. Conf. on High Energy Physics, Osaka (2000), eds. C.S. Lim and T. Yamanaka.

[9] K. Sliwa, S. Riley and U. Baur, ATLAS, ATL-PHYS-2000-018.

[10] C.K. Mackay, P.R. Hobson, CMS NOTE-2001/052 and CMS NOTE-2001/056.

[11] C.K. Mackay, P.R. Hobson, CMS NOTE-2002/028.

[12] J.J. van der Bij, A. Ghinculov, hep-ph/9909409.

[13] M. Dobbs, talk at the 15th Topical Conference on Hadron Collider Physics 2004, East Lansing.

[14] O. Eboli, M Gonzalez-Garcia, S. Lietti, S. Novaes, Phys. Rev. D63 (2001), 075008.

[15] I. Borjanovic, SN-ATLAS-2004-040.

[16] L. Sonnenschein, CMS NOTE-2001/001.

[17] A. Kharchilava, CMS NOTE-1999/065.

[18] CDF collab., T. Affolder et al., Phys. Rev. Lett 84, 216 (2000); D0 collab., V.M. Abrazov et al., hep-ex/0404040, subm. to Phys. Rev. Lett.

[19] L.Sonnenschein, thesis RWTH Aachen, May 2001, PITHA 01/04.

[20] M. Ciljak et. al., ATLAS, ATL-PHYS-2003-035.